TiO_2 NPs improve ultrasound response: CS/β-GP/TiO_2 NP hydrogel enabling on-demand administration

YUE ZHOU[1], YI-RAN YAO[1], YAN XU[1], XIN RONG[1], YUE-FENG QIU[2] and TING-YUE QI[1]

[1]Department of Ultrasound, Medical Imaging Center, Affiliated Hospital of Yangzhou University, Yangzhou University, Yangzhou, Jiangsu 225012, P.R. China; [2]College of Chemical Engineering, Nanjing Tech University, Nanjing, Jiangsu 211816, P.R. China

Received October 8, 2024; Accepted March 17, 2025

DOI: 10.3892/br.2025.2020

Abstract. The present study developed a novel injectable, biocompatible, and thermosensitive hydrogel system for ultrasound-triggered drug release, using a chitosan/sodium β-glycerophosphate/titanium dioxide nanoparticle (CS/β-GP/TiO_2 NP) composite. The inclusion of TiO_2 NPs aimed to enhance ultrasound sensitivity, enabling precise therapeutic release to targeted tissues. The hydrogels displayed excellent injectability (maximum injection force <6.5 N) and gelled effectively at body temperature. Biocompatibility was confirmed through Cell Counting Kit-8, LIVE/DEAD, and western blot assays. The present study demonstrated that hydrogels with TiO_2 NPs significantly increased the release rates of sodium fluorescein and bovine serum albumin, affirming the role of TiO_2 NPs as a sensitizer. This establishes the CS/β-GP/TiO_2 NP hydrogel as a promising system for ultrasound-responsive drug delivery. Potential applications include drug delivery, tissue engineering, and wound healing, with the system offering controlled and targeted therapy under ultrasound stimulation. Future research will optimize hydrogel properties, assess *in vivo* performance, and evaluate long-term stability and effectiveness in clinical settings.

Introduction

The administration of medication to patients, which often necessitates controlled and sustained delivery over predefined time intervals, is accomplished through drug delivery systems (1). In addition to minimizing dosage, such systems can reduce dosing frequency. Water-based hydrogels, characterized by low protein adhesion and a diminished propensity for inflammatory responses, have been extensively used in drug delivery systems. However, the conventional implantation of hydrogels via surgical procedures may inflict considerable trauma. Recent studies focused on the development of minimally invasive injectable hydrogels (2,3).

Medications are encapsulated within drug delivery systems and subsequently released into their pertinent matrices. Furthermore, researchers have discovered avenues to impart responsiveness to drug delivery systems, such as light stimulation (4), pH modulation (5), ultrasound activation (6), and thermal triggers (7), achieving 'on-demand' drug release. Compared with other stimuli, ultrasound presents the advantages of affordability, non-invasiveness, and rapid response kinetics when acting as a triggering modality. Ultrasound has been substantiated as an effective means of motivating hydrogels to release drugs and has been widely applied in various diseases, including cancer, fractures, thrombosis and infections (8).

Chitosan (CS), a natural alkaline polysaccharide, has gained extensive attention in medical research owing to its biocompatibility, biodegradability in both intra- and extracorporeal environments, and notable antibacterial properties (9). In this context, the present study delves into the ultrasonic response performance of the CS/sodium β-glycerophosphate (β-GP) composite as a model for the temperature-sensitive hydrogel. Crosslinked by physical means, this hydrogel can both possess the ability to transition from liquid states to gel states at body temperature and preserve its inherent characteristic, thus imparting ideal attributes for injectability.

A challenge in the advancement of ultrasound-responsive hydrogels lies in the fact that numerous hydrogel matrices have been regularly observed to have low ultrasound adsorption capacity, which results in diminished responsiveness to ultrasound. Researchers have explored the augmentation of hydrogel ultrasound responsiveness by incorporating sonosensitizers (6). These sonosensitizers include organic compounds such as porphyrin derivatives and phthalocyanines, as well as inorganic compounds such as calcium carbonate and titanium dioxide. However, conventional organic sonosensitizers have shortcomings such as toxicity, poor water solubility, and suboptimal utilization (10).

To address these challenges, the present study opts to add titanium dioxide nanoparticles (TiO_2 NPs) as a sonosensitizer into the CS/β-GP temperature-sensitive hydrogel. The

Correspondence to: Professor Ting-Yue Qi, Department of Ultrasound, Medical Imaging Center, Affiliated Hospital of Yangzhou University, Yangzhou University, 368 Hanjiang Middle Road, Hanjiang, Yangzhou, Jiangsu 225012, P.R. China
E-mail: tyqi@yzu.edu.cn

Key words: ultrasound response, injectable, drug release, titanium dioxide nanoparticles

selection was based on the advantageous attributes of TiO_2 NPs, including improved biocompatibility and water solubility, compared to those of traditional organic alternatives. The incorporation of this sonosensitizer was anticipated to elevate the ultrasound responsiveness of the hydrogel, and its performance was evaluated through simulated release studies involving both small- and large-molecule drugs.

Materials and methods

Materials and apparatus

Experimental materials. The following materials were used: i) CS powder (95% deacetylation degree; cat. no. C105799; Aladdin Scientific Corp.), ii) β-GP pentahydrate (cat. no. D106347; Aladdin Scientific Corp.), iii) sodium fluorescein (NaF; cat. no. F105615; Aladdin), iv) TiO_2 NPs (20-40 nm; cat. no. NM000800; Beijing Solarbio Science & Technology Co., Ltd.), v) L929 murine fibroblast cells (cat. no. KGG1306-1), vi) RPMI-1640 medium (containing newborn calf serum, double antibiotics; cat. no. KGL1509-500), vii) Cell Counting Kit-8 (CCK-8) cell proliferation assay kit (cat. no. KGA9305-500), viii) LIVE/DEAD cell viability assay kit (cat. no. KGA9501-1000), ix) bovine serum albumin (BSA) (standard grade, heat-treated) (cat. no. KGL2314-10), x) bicinchoninic acid (BCA) protein quantification assay kit (cat. no. KGB2101-250), all from Jiangsu KeyGen Biotech Co., Ltd., xi) mouse anti-proliferating cell nuclear antigen (PCNA) antibody (1:1,000; cat. no. BM0104) and xii) goat anti-mouse IgG/HRP antibody (1:10,000; cat. no. BA1056) both from Boster Biological Technology Co. Ltd.

Experimental apparatus. The primary apparatus were the following: i) CO_2 cell culture incubator, ii) laboratory heating magnetic stirrer, iii) Fourier-transform infrared spectrometer (Nicolet 8700; Thermo Fisher Scientific, Inc.), iv) rheometer (TA Instruments), v) inverted fluorescence microscope (Zeiss GmbH); vi) electrophoresis system, vii) blotting apparatus (Bio-Rad Laboratories, Inc.), viii) automated digital gel imaging system (Tanon GIS 2010; Tanon Science and Technology Co., Ltd.), ix) LAS X4.4.0 (Leica Microsystems GmbH), x) microplate reader (Anthos ht2; Anthos Labtec), xi) mechanical testing machine (ZwickRoell; Zwick GmbH & Co.) and xii) Vibra-Cell™ ultrasonic disruptor (Sonics & Materials, Inc.).

Methods

Preparation of hydrogels

Preparation of CS solution. CS powder (95% deacetylation degree) was dissolved in an ice acetic acid solution (2% w/v concentration in 0.1 mol/l solution). The mixture was stirred at 25˚C overnight until complete dissolution. After filtration through a 150-mesh silk screen, the solution was allowed to stand and underwent high-pressure steam sterilization (151˚C for 15 min), followed by storage at 4˚C.

Preparation of β-GP solution. *β-GP* powder (5.6 g) was dissolved at a concentration of 56% w/v in deionized water, stirred at room temperature for 10 min until complete dissolution, and then sterilized by filtration through a 0.2-*μ*m filter. The solution was stored at 4˚C.

Preparation of TiO_2 NP solution. After 6 h of ultraviolet sterilization, the TiO_2 NP powder was added to deionized water at a concentration of 1% w/v. The mixture was sonicated (the ultrasonic power was 240W) to obtain a uniform dispersion and was immediately used.

CS/β-GP/TiO_2 NP hydrogel preparation. The CS solution was then stirred in an ice bath using a magnetic stirrer. The β-GP solution was added dropwise in a 9:1 ratio, followed by continuous stirring at room temperature for 10 min. Subsequently, different proportions (0, 0.5, 1, and 1.5%) of TiO_2 NP solution were added dropwise to the prepared CS/β-GP solution, followed by 20 min of stirring at room temperature. The mixture was sealed and placed in a 37˚C water bath incubator to solidify for 24 h.

Chemical characterization. Fourier-transform infrared spectroscopy (FTIR) was used to analyze the formation of copolymers in the hydrogels. Hydrogels with varying contents of TiO_2 NPs were prepared, and FTIR was conducted in the wavelength range of 400-4,000 cm^{-1} with four scans obtained per sample. The scanning resolution was set at 4 cm^{-1}, and the scanning speed was 0.2 mm/sec.

Rheological analysis. Hydrogels with varying TiO_2 NP content were analyzed using a rheometer with a cone and plate geometry featuring a cone angle of 2˚, a diameter of 20 mm, and a gap of 0.054 mm. The plate was equilibrated to the initial temperature (25˚C), and a temperature ramp test was performed in the range of 25-50˚C, for 250 min. The ramp rate was 0.1˚C/min, the frequency was 1.5 Hz, the shear strain was controlled at 1%, and the angular frequency was set to 10 rad/sec. Data were collected every second to determine solid-state transition temperatures. Cold traps were employed in all the rheometers to minimize solvent evaporation.

Injectable property of hydrogels. The injectability of the hydrogel was evaluated using a mechanical testing machine equipped with a 5 kN load cell. During the test, 10 ml of each hydrogel were loaded into a custom injection mold. The test was conducted at room temperature with a displacement of 5 mm and a crosshead speed of 30 mm/min, simulating the speed of manually injecting the hydrogel from a syringe. Each experiment was repeated three times to ensure accuracy and reliability. The load required as function of piston displacement was measured, and the average maximum force value for each composition was determined.

Assessment of hydrogel biocompatibility

Cell proliferation toxicity test (CCK-8 assay). L929 murine fibroblast cells were cultured in RPMI-1640 medium containing 10% fetal bovine serum and 1% double antibiotics, according to the manufacturer's instructions. Upon reaching 90% confluence, cells were trypsinized and passaged during the logarithmic growth phase. L929 cells were seeded at a density of $4x10^3$ cells/well in 96-well plates. After 24 h of culture under 37˚C and 5% CO_2, the original culture medium was aspirated. The control group received 100 *μ*l RPMI-1640 medium, while the other groups were treated with 90 *μ*l RPMI-1640 medium (containing fetal bovine serum and double antibiotics) along with 10 *μ*l of different concentrations of CS/β-GP/TiO_2 NP

Table I. Ultrasound treatment regimes.

Ultrasound treatment groups	Ultrasound treatment 1	Ultrasound treatment 2	Ultrasound treatment 3
Treatment details	Ultrasound applied in 2.5-min pulses once per hour for 5 h	Ultrasound applied in 2.5-min pulses once per hour for 5 h following an initial 24-h immersion period	Ultrasound applied in 2.5-min pulses once per hour for 5 h following an initial 72-h immersion period

Ultrasound with an intensity of 9.6 mW/cm^2 was applied in 2.5-min pulses, once per hour for a 5-h period. For ultrasound treatment 1, the ultrasound regime was applied at 0 h; for ultrasound treatment 2, it was applied after incubation for 24 h; and for ultrasound treatment 3, it was applied after incubation for 72 h.

hydrogel (0, 0.5, 1 and 1.5%). On days 1, 3, 5 and 7, the CCK-8 cell proliferation toxicity assay was performed (concentration, 10%). The supernatants were collected, and the optical density (OD) at a wavelength of 450 nm was measured using an ELISA reader.

Cell viability and cytotoxicity staining. L929 cells were seeded at a density of 8x10^3 cells/well in a 96-well plate. After 24 h of culture under 37˚C and 5% CO_2, the original culture medium was aspirated. The control group received 100 μl RPMI-1640 medium, while the other groups were treated with 90 μl RPMI-1640 medium (containing fetal bovine serum and double antibiotics) along with 10 μl of different concentrations of CS/β-GP/TiO_2 NP hydrogel (0, 0.5, 1 and 1.5%). After 24 h of incubation at 37˚C, the cells were stained using Calcein-AM and PI dyes (included in the LIVE/DEAD cell viability assay kit). The cells were incubated with the staining solution for 2 h at 37˚C and observed under an inverted fluorescence microscope at an excitation wavelength of 490 nm for live cells and 545 nm for dead cells.

Western blot analysis. L929 cells in good growth condition were seeded at a density of 5x10^5 cells/well in 6-well plates. When cell growth reached 80-90% confluence, the intervention groups were treated with 200 μl of CS/β-GP/TiO_2 NP hydrogel (0, 0.5, 1 and 1.5%) along with 1.8 ml of RPMI-1640 medium. The control group received 2 ml of the medium solution. After 24 h of incubation, the total cellular protein was extracted using Cell Lysis Buffer for Western or IP (cat. no. P0013; Beyotime Insitute of Biotechnology), and the protein concentration was determined using a BCA protein quantification assay kit. Samples were boiled in 5X loading buffer for 10 min. For western blot analysis, 20 μg of protein was loaded per lane to ensure consistent sample loading. Electrophoresed at 80 V at a constant voltage until they entered the separating gel (10%), and then transferred to a PVDF membrane. The membrane was blocked with TBST buffer containing 5% skim milk powder at room temperature for 1 h. Mouse anti-PCNA antibody (1:1,000) was added and incubated overnight at 4˚C. After washing the membrane with TBST (including 0.1% Tween-20), goat anti-mouse IgG/HRP antibody (1:10,000) was added and the membrane was incubated for 1 h at 4˚C. Protein expression was detected using a highly sensitive ECL luminescence reagent (Epizyme Biomedical Technology). β-actin (cat. no. BA2305; Boster Biological Technology Co., Ltd.) was used as the reference protein. ImageJ 1.45 (National Institutes of Health) was used for densitometric analysis. PCNA is a sensitive and specific marker of cell proliferation, capable of accurately reflecting the proliferative activity of cells. It has been widely used in biocompatibility studies of various biomaterials, especially in the fields of tissue engineering and regenerative medicine (11-14).

Ultrasound-triggered simulated drug release

Ultrasound-triggered release of NaF from CS/β-GP/TiO_2 NP hydrogel. NaF, a water-soluble fluorescent dye, was used as a small-molecule drug analog to assess the ultrasound-controlled release of the hydrogel. Two hydrogel formulations were evaluated: i) CS/β-GP and ii) CS/β-GP/TiO_2 NPs containing 1.5% TiO_2 NPs. A total of 10 mg of NaF salt were added to 10 ml of double-distilled water, resulting in a NaF solution with a concentration of 1 mg/ml. During the preparation of composite hydrogels, the NaF solution was incorporated into the hydrogel mixture at a ratio of 100 μl/ml before mixing β-GP into the hydrogels, ensuring the uniform distribution of NaF. For release studies, a 1-ml sample of the hydrogel was immersed in 5 ml of a buffer medium consisting of 0.01 M calcium- and magnesium-free Dulbecco's phosphate-buffered saline (DPBS; cat. no. KGL2208-500; Jiangsu KeyGen Biotech Co., Ltd.) at pH 7.4 and maintained at 37˚C throughout the testing period. The diffusion-mediated release of NaF was evaluated at 0, 5, and 24 h after incubation without ultrasound treatment.

The ultrasound treatment was performed as revealed in Table I. The approach involved applying ultrasound for 5 h at time point 0 (ultrasound intensity=9.6 mW/cm^2; 25% amplitude; 2.5 min/h; 37˚C; 5-h cycles). This scheme was based on previous studies conducted by Huebsch *et al* (15) and Levingstone *et al* (16). The amount of NaF released after ultrasound application was compared with the control group without ultrasound treatment at the 5-h time point. At each time point, 1 ml of the supernatant was collected, and the absorbance at 512 nm was measured using an ELISA reader to assess the NaF concentration.

Ultrasound-triggered release of BSA from CS/β-GP/TiO_2 NP hydrogel. Subsequently, the ultrasound-controlled release of BSA was investigated as a large-molecule drug/protein analog. For BSA release studies, two hydrogel compositions were tested: i) CS/β-GP and ii) CS/β-GP/TiO_2 NPs containing 1.5% TiO_2 NPs, prepared as aforementioned. BSA was added to double-distilled water to achieve a concentration of 10 mg/ml and then added to the hydrogel to create a 1 mg/ml BSA solution. Subsequently, 1 ml of the hydrogel sample was

suspended in a buffer medium containing 5 ml of 0.01 M calcium-magnesium-free DPBS at pH 7.4 and 37˚C.

Release studies were conducted at 0, 5, 24, 29, 72 and 77 h without ultrasound application. Ultrasound treatment was performed using three different approaches, as shown in Table I. For the first ultrasound treatment, ultrasound was applied for 5 h at time point 0 (ultrasound intensity=9.6 mW/cm^2; 25% amplitude; 2.5 min/h; 37˚C; 5-h cycles) (15,16). For the second ultrasound treatment, hydrogels were incubated for 24 h at 37˚C, followed by 5-h ultrasound treatment using the first ultrasound treatment protocol. For the third ultrasound treatment, hydrogels were incubated for 72 h at 37˚C, followed by 5-h ultrasound treatment using the first protocol. The results at the same time points were compared with those of the diffusion-based release control group without ultrasound treatment.

BSA was quantified using a BCA protein quantification assay kit. The assay was conducted according to the manufacturer's instructions, and the absorbance at 562 nm was measured using an ELISA reader to determine BSA concentration.

Statistical analysis. Unless otherwise specified, the experiments were conducted in triplicate. The data results were generally reported as the mean ± standard deviation (SD) and analyzed statistically based on this format. Statistical analyses were performed using GraphPad Prism 8 software (GraphPad; Dotmatics) and SPSS 25.0 (IBM Corp.). Statistical significance was determined using the unpaired t-test and one-way analysis of variance (ANOVA). Tukey's post hoc test was used after ANOVA. $P<0.05$ was considered to indicate a statistically significant dofference.

Results

Preparation of composite hydrogels. Composite hydrogels with TiO_2 NP contents of 0, 0.5, 1, and 1.5% in CS/β-GP/TiO_2 NPs were successfully synthesized.

Chemical characteristics of composite hydrogels. Characterization analysis of pure CS/β-GP and CS/β-GP/TiO_2 NPs was conducted using FTIR, confirming the successful incorporation of TiO_2 NPs at different concentrations into the hydrogels (Fig. 1). The wide absorption peak at 3,600-3,200 cm^{-1} corresponded to the stretching vibrations of hydroxyl groups (O-H) and amino groups (N-H). The peaks at 2,932 and 2,856 cm^{-1} represented the antisymmetric and symmetric stretching vibrations of methylene groups (CH_2), respectively. The absorption peak at 1,648 cm^{-1} corresponded to the amide I band stretching vibration of C=O. The peak at 1,557 cm^{-1} corresponded to the bending vibration of C-N-H in the amide II band. The peak at 1,384 cm^{-1} corresponded to the symmetric bending vibration of methyl groups (C-CH_3). The peaks at 1,122 and 1,079 cm^{-1} corresponded to the stretching vibrations of C-O, while those at 1,079 and 974 cm^{-1} corresponded to the antisymmetric and symmetric stretching vibrations of phosphate groups, respectively. The peak at 783 cm^{-1} was possibly associated with the swinging vibration of C-H.

With increasing TiO_2 NP content, the absorption peak at 3,600-3,200 cm^{-1} broadened, indicating the introduction of more hydroxyl groups (O-H), possibly owing to the residual water in TiO_2 NPs. The absorption peak of the amide I band

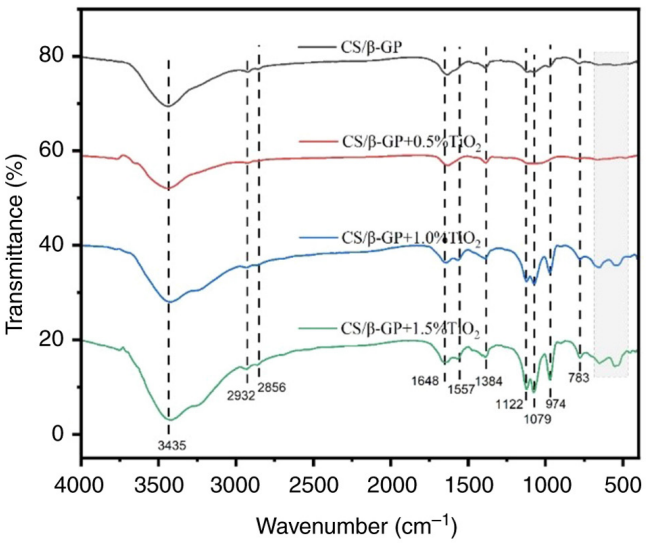

Figure 1. Fourier transform infrared spectroscopy for thermally responsive hydrogels, showing the incorporation of TiO_2 NPs into the CS/β-GP co-polymer. TiO_2 NPs, titanium dioxide nanoparticles; CS/β-GP, chitosan/β-glycerophosphate.

C=O stretching vibration shifted from 1,628 cm^{-1} to 1,648 cm^{-1}, indicating a blue shift. The peaks at 1,557 cm^{-1}, 1,384 cm^{-1}, and 1,300-700 cm^{-1} intensified, which might be attributed to the vibrations of organic compounds present in TiO_2 NPs. New absorption peaks appeared at 500-700 cm^{-1}, possibly corresponding to the stretching and bending vibrations of Ti-O in the introduced TiO_2 NPs.

Rheological analysis. The thermal response characteristics of all the hydrogels were evaluated by rheological analysis. The solidification temperatures of pure CS/β-GP hydrogel and hydrogels with added TiO_2 NPs were found to be in the range of 36.5-37.3˚C (Fig. 2).

Injectable properties of composite hydrogels. Injectability experiments were conducted to assess the feasibility of the prepared hydrogels as clinical injection materials. No significant differences in the injection forces between the four hydrogel groups were observed (Fig. 3). The injection force for the CS/β-GP group was 5.79±0.57 N, for the CS/β-GP + 0.5% TiO_2 NP group it was 5.63±0.41 N, for the CS/β-GP + 1.0% TiO_2 NP group it was 5.54±0.67 N, and for the CS/β-GP + 1.5% TiO_2 NP group it was 5.70±0.49 N. Additionally, all these values were lower than the maximum force (22.6 N) that a surgeon's hand can comfortably apply to an injector (17). This indicates that all the hydrogel formulations prepared were suitable for use as injection materials in a clinical setting.

Biocompatibility assessment of hydrogels

CCK-8 assay. The doubling time of L929 cells is generally 28-36 h. In the present experiment, the number of L929 cells increased by only ~2-fold over 7 days, which is indeed lower than the typically expected proliferation rate. It is considered that the possible reasons for this could be the use of a different culture medium or a lower initial cell density at the beginning

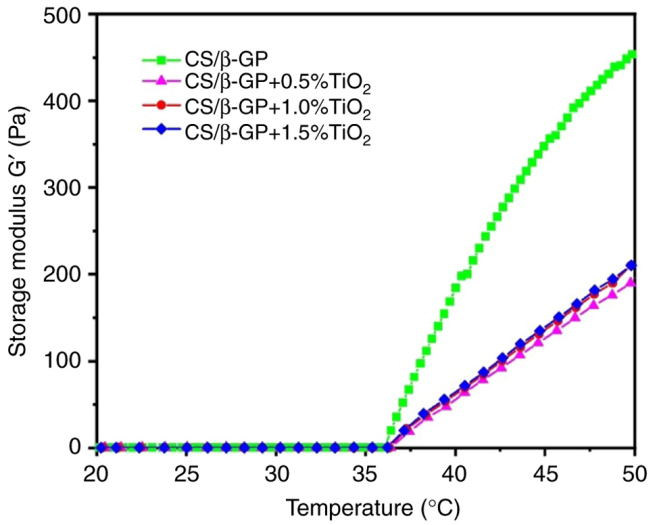

Figure 2. Storage modulus as a function of TiO_2 NP concentration from 20 to 50˚C indicating the low critical solution temperature transition points from liquid to solid state. TiO_2 NPs, titanium dioxide nanoparticles; CS/β-GP, chitosan/β-glycerophosphate. Figure 2. Storage modulus as a function of TiO_2 NP concentration from 20 to 50˚C indicating the low critical solution temperature transition points from liquid to solid state. TiO_2 NPs, titanium dioxide nanoparticles; CS/β-GP, chitosan/β-glycerophosphate.

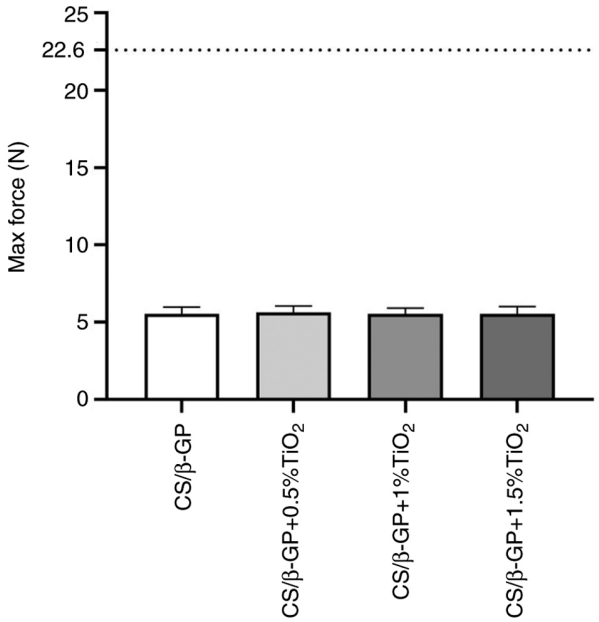

Figure 3. Injectability of the pure CS/β-GP hydrogel and thermally responsive hydrogels containing 0.5, 1.0 and 1.5% wt./vol. TiO_2 NPs. No significant difference was observed between groups. The forces recorded for all hydrogels were below the maximum force that can be comfortably applied to a syringe by a surgeon's hand, highlighted on the graph at 22.6 N. TiO_2 NPs, titanium dioxide nanoparticles; CS/β-GP, chitosan/β-glycerophosphate.

of the experiment. The cell count increased over time, and the absorbance values at various time points after seeding the cells onto different composite hydrogels were not significantly different from those of the control group, which was cultured in conventional plastic 96-well plates (Fig. 4). There were no statistically significant differences between the groups (P>0.05).

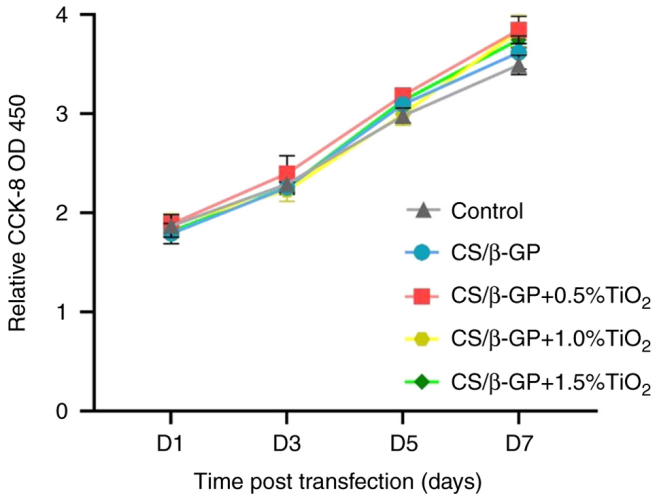

Figure 4. CCK-8 assays of different composite hydrogels. Different composite hydrogels were not significantly different from the control group by CCK-8 assay. There were no statistically significant differences (P>0.05). CCK-8, Cell Counting Kit-8; OD, optical density; CS/β-GP, chitosan/β-glycerophosphate; TiO_2 NPs, titanium dioxide nanoparticles.

Cell viability and cytotoxicity staining. Cell viability staining accurately distinguished live from dead cells on the material surface. The survival rates of cells co-cultured with various hydrogel formulations were not significantly different from those of the control group (Fig. 5), which were consistent with the CCK-8 results. Both the CCK-8 assay and cell viability staining indicated that the prepared composite hydrogels exhibited excellent biocompatibility. Due to the experimental results showing a very clear distinction between live and dead cells, with almost no dead cells detected across all groups and a live cell proportion close to 100%, further quantitative analysis was not conducted.

Western blot analysis. After co-culturing L929 cells with various hydrogel groups for 24 h, western blot analysis was performed to assess protein PCNA expression. No significant differences in cellular protein expression among the different groups were observed (P>0.05) (Fig. 6).

Considering the results from the injectability test, the CCK-8 cell proliferation assay, the cell viability staining experiment, and given that all CS/β-GP and TiO_2 NP polymer composites exhibited the required properties for injectable hydrogels and showed no cell toxicity, the CS/β-GP + 1.5% TiO_2 NP hydrogel was selected for further investigation into ultrasound-triggered drug release. This hydrogel was opted due to the high percentage of the sonosensitizer TiO_2 NPs.

Ultrasound-triggered simulated drug release

Release of NaF from CS/β-GP/TiO_2 NP hydrogels upon ultrasound stimulation. The release of NaF from CS/β-GP and CS/β-GP + 1.5% TiO_2 NP thermosensitive hydrogels upon ultrasound stimulation was evaluated. When hydrogel samples were suspended in DPBS at 37˚C, the hydrogel remained in a gel state. After treatment with an ultrasonic disruptor, the main changes observed in the hydrogel samples were local structural damage or disintegration, rather than complete dissolution. The analysis of diffusion-related release for each

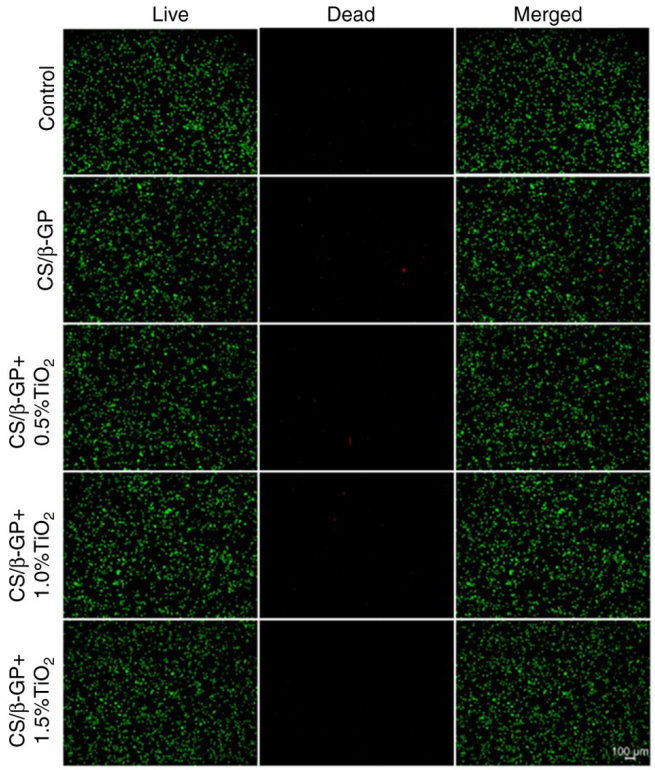

Figure 5. Survival rates of different composite hydrogels. The survival rates of cells co-cultured with various hydrogel formulations were not significantly different from the those of the control group, as assessed by LIVE/DEAD assay. CS/β-GP, chitosan/β-glycerophosphate; TiO_2 NPs, titanium dioxide nanoparticles.

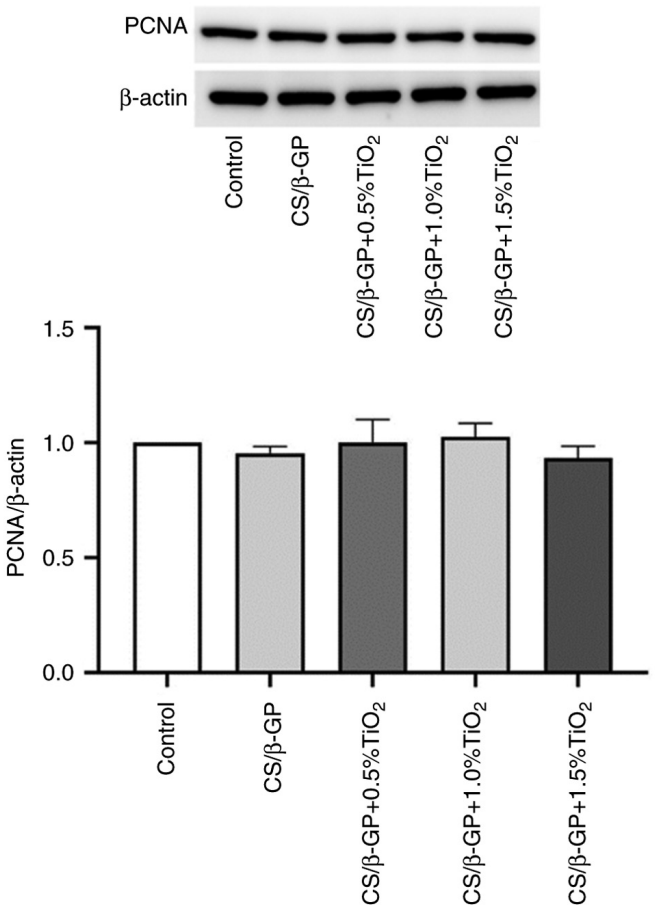

Figure 6. Western blotting results of different composite hydrogels. The results of western blotting assay revealed no significant differences in cell protein expression among the different groups (P>0.05). PCNA, proliferating cell nuclear antigen; CS/β-GP, chitosan/β-glycerophosphate; TiO_2 NPs, titanium dioxide nanoparticles.

hydrogel group revealed that NaF was gradually released over time, with up to 33.15±0.89% release observed within 24 h solely due to diffusion. At the 0 and 5-h time points, the incorporation of TiO_2 NPs into the thermo-responsive hydrogel had no significant impact on the NaF diffusion-related release. However, at the 24-h time point, the NaF release level from the CS/β-GP + 1.5% TiO_2 NP group was significantly lower than that from the CS/β-GP group (P<0.01) (Fig. 7A). This suggests that hydrogels containing TiO_2 NPs may reduce diffusion-related NaF release. Ultrasound increased the release of NaF from both hydrogel groups. For the CS/β-GP group, ultrasound treatment method 1 resulted in 24.16±1.32% NaF release, significantly increasing NaF release compared with the control group at the same time point (5 h; 16.05±0.07%; P<0.01). For the CS/β-GP + 1.5% TiO_2 NP group, the first ultrasound treatment method led to 27.77±0.98% NaF release, significantly increasing NaF release compared with the control group at the same time point (18.21±0.48%; P<0.01). Furthermore, using the first ultrasound treatment method, the release of NaF from the CS/β-GP + 1.5% TiO_2 NP group was significantly higher than that from the CS/β-GP group (P<0.01) (Fig. 7B).

Release of BSA from CS/β-GP/TiO_2 NP hydrogels upon ultrasound stimulation. The ultrasound-triggered release of BSA was evaluated for CS/β-GP and CS/β-GP + 1.5% TiO_2 NP hydrogels. The analysis of diffusion-related BSA release for each hydrogel group revealed relatively low BSA release levels over time, with 6.63±0.50% and 6.97±0.30% BSA released from CS/β-GP and CS/β-GP + 1.5% TiO_2 NP groups, respectively, at the 72-h time point (Fig. 8A). No significant differences in diffusion-related BSA release between CS/β-GP and CS/β-GP + 1.5% TiO_2 NP groups was observed. And under the experimental conditions, no significant degradation or disintegration of the hydrogel network was observed within 72 h. The physical integrity of the hydrogels remained intact. Ultrasound application increased the release of BSA from pure CS/β-GP and CS/β-GP + 1.5% TiO_2 NP hydrogels. For the CS/β-GP hydrogel, the BSA release recorded after ultrasound treatment method 1 was 24.94±1.82% (Fig. 8B), which was significantly higher than that for the control group at the same time point (5 h), which released only 3.46±0.34% BSA. Compared with the BSA level recorded for the first ultrasound treatment method, the levels recorded for the second and third ultrasound treatment methods were slightly lower, possibly due to BSA degradation over time. Notably, in the first ultrasound treatment method, the incorporation of TiO_2 NPs into the thermo-responsive hydrogel increased BSA release, with the CS/β-GP + 1.5% TiO_2 NP group releasing 49.42±0.55%, which was significantly higher than the release from the CS/β-GP group (24.94±1.82%). Similar increases were observed for the second and third ultrasound treatment method (Fig. 8C and D).

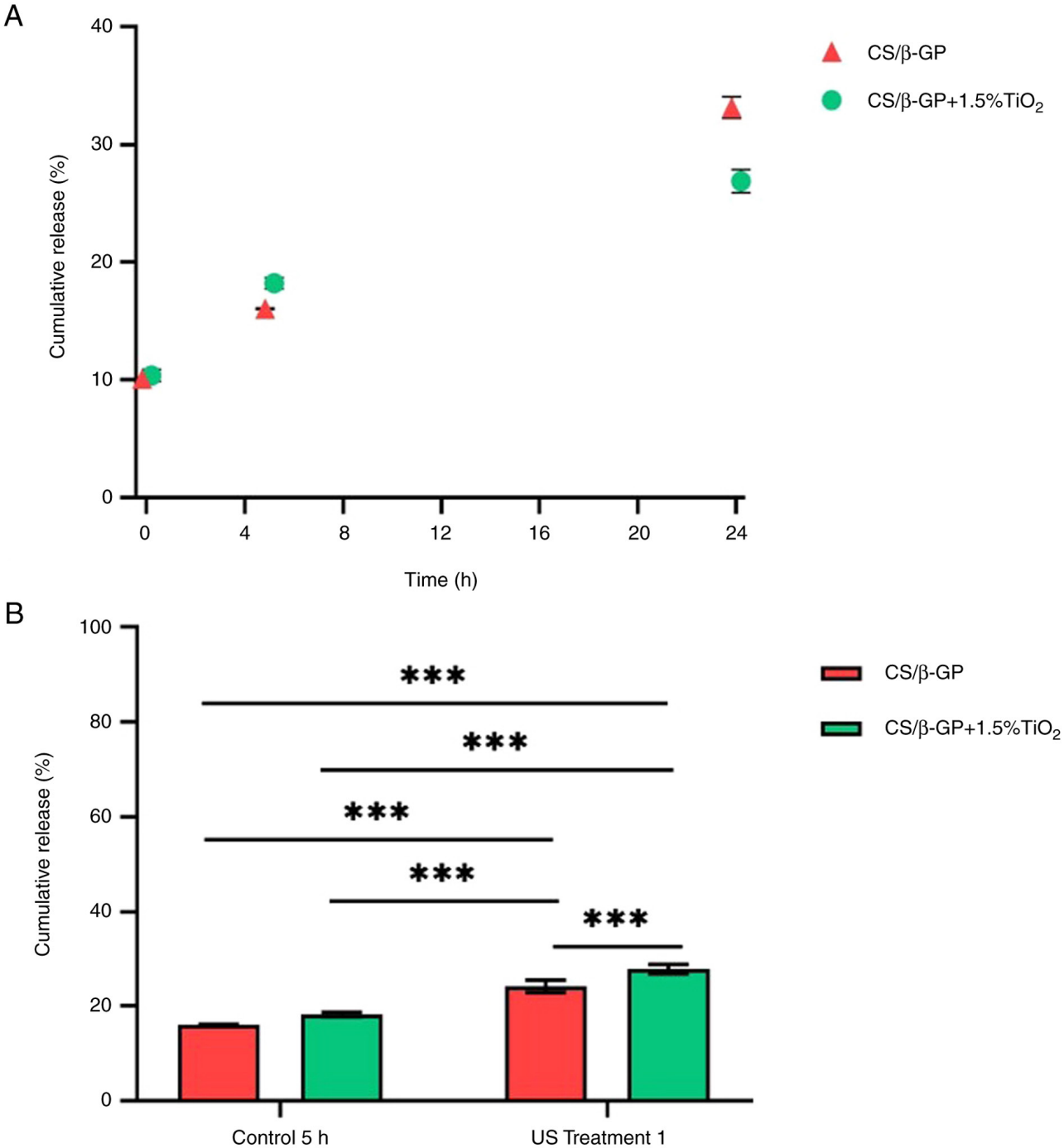

Figure 7. Cumulative release of NaF from NaF-loaded thermally responsive hydrogels. (A) Diffusion-related release of NaF from the pure CS/β-GP and CS/β-GP + 1.5% TiO_2 NP groups up to 24 h. (B) Ultrasound triggered release of NaF following the first ultrasound treatment. ***P<0.001. NaF, sodium fluorescein; CS/β-GP, chitosan/β-glycerophosphate; TiO_2 NPs, titanium dioxide nanoparticles.

Discussion

The development of minimally invasive systems for precise control of therapeutic delivery holds significant promise for drug administration applications. To address this need, a biocompatible and thermosensitive hydrogel system was developed as a delivery platform. This dual-stimulus system allows for the minimally invasive delivery of hydrogels that gel *in situ* at body temperature and then release therapeutic agents or drugs on demand through ultrasound waves. In the present study, the release of NaF and BSA mimics from CS/β-GP and CS/β-GP/TiO_2 NP hydrogels was controlled by ultrasound. The results demonstrated that the inclusion of TiO_2 NPs as a sensitizer enhanced the ultrasound-responsive capability of hydrogels, leading to an increased release of the mimics.

This hydrogel exhibits significant thermosensitivity, which can be regulated by temperature changes. This characteristic makes it highly promising for applications such as controlled drug release (18), tissue engineering (19), and biosensors (20). As the temperature increases, the hydrogel undergoes a phase transition, altering its swelling behavior and mechanical properties. This reversible temperature-responsive feature allows

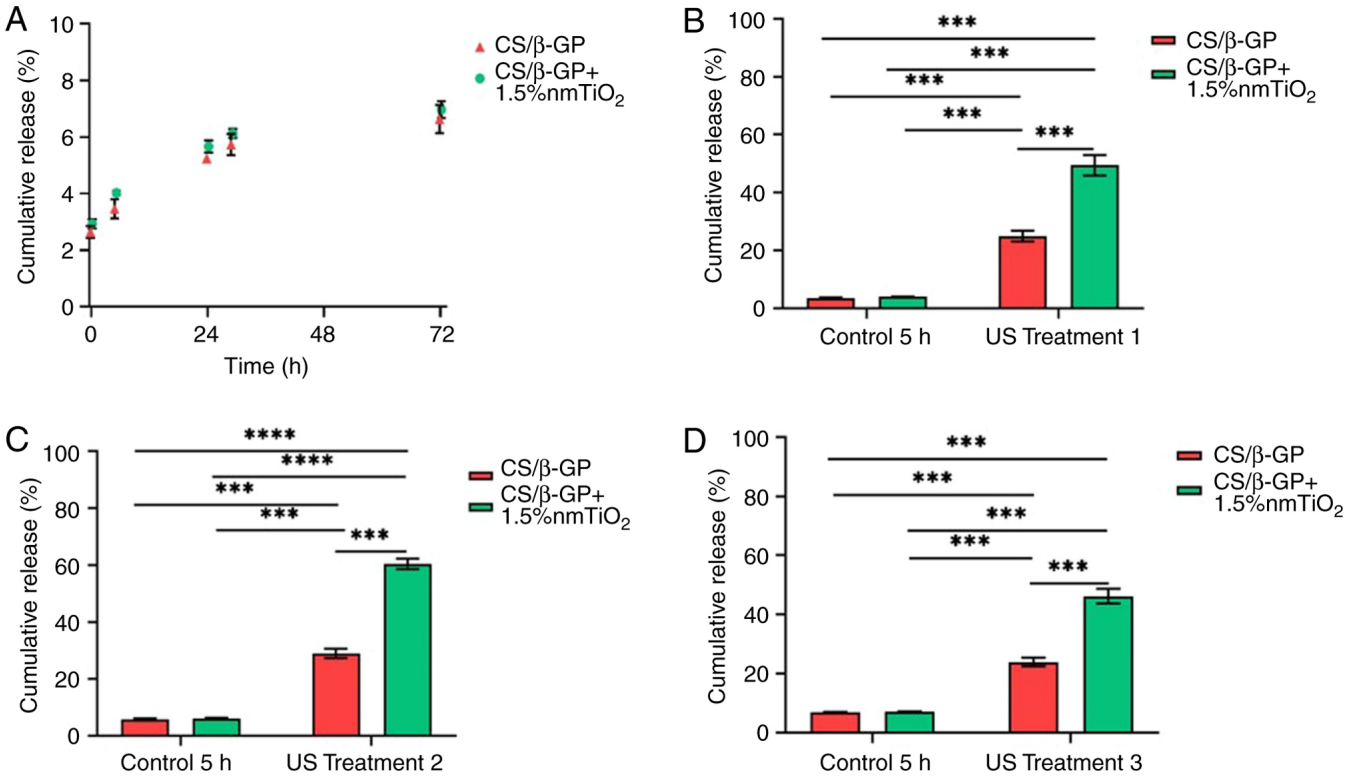

Figure 8. Cumulative release of BSA from BSA loaded thermally responsive hydrogels. (A) Diffusion related release of pure CS/β-GP and CS/β-GP + 1.5% TiO_2 NP groups up to 72 h. Ultrasound-triggered release of BSA is shown following (B) first ultrasound treatment, (C) second ultrasound treatment and (D) third ultrasound treatment. ***P<0.001 and ****P<0.0001. BSA, bovine serum albumin; CS/β-GP, chitosan/β-glycerophosphate; TiO_2 NPs, titanium dioxide nanoparticles.

the hydrogel to achieve desired functions under specific conditions. For instance, in drug delivery systems, by adjusting the temperature, the release rate and dosage of the drug can be controlled, achieving precise drug delivery.

Various biocompatible hydrogels with excellent drug-loading capacities have been widely used in drug delivery applications (21-23). Implanting such hydrogels into the human body in a minimally invasive manner would likely be better accepted by patients. Injectable biomaterials that can transition from liquid to solid in response to specific stimuli are highly attractive for clinical use (24,25). The therapeutic targets within the human body often have irregular shapes that can be initially filled as a liquid in the form of a thermoresponsive hydrogel and then transformed into a gel state at a physiological temperature after injection. In addition to the sustained slow release after implantation, the intermittent release of bioactive compounds may also be necessary for certain biological effects. Thus, the platform should possess features of external stimulus responsiveness to achieve a scenario-based release (26). Acoustic-responsive scaffolds have been designed with the potential for controlled release (27). CS is a naturally biodegradable and biocompatible polymer that has shown promise for various applications (28). Incorporating β-GP into CS to create a composite hydrogel has been shown to yield a thermo-responsive hydrogel. In the present study, the addition of TiO_2 NPs to CS/β-GP hydrogel was demonstrated to have no negative impact on its thermal responsiveness through rheological analysis. Through CCK-8 experiments, LIVE/DEAD staining, and western blot experiments, the biocompatibility of CS/β-GP and CS/β-GP/TiO_2 NP hydrogels was confirmed, rendering them suitable for clinical research.

Ultrasound-triggered release of loaded molecules from thermo-responsive CS/β-GP hydrogels, with or without TiO_2 NPs, was studied. First, the release of the small-molecule drug mimic NaF and large-molecule mimic BSA from two thermo-responsive hydrogel compositions (CS/β-GP and CS/β-GP/TiO_2 NPs) was assessed. The release of the mimics from both hydrogel groups was higher with the ultrasound treatment than with the untreated control, and hydrogels containing TiO_2 NPs exhibited more significant ultrasound-responsive capability, releasing more mimics than the CS/β-GP group after ultrasound treatment. This demonstrated that the addition of TiO_2 NPs to CS/β-GP hydrogel confered ultrasound-responsive capabilities on a biocompatible basis.

The results of the present study highlight the need to develop a novel dual-stimulus delivery system for drug delivery. The results indicate that successful inclusion of TiO_2 NPs into CS/β-GP hydrogel creates a thermo-responsive hydrogel suitable for minimally invasive delivery. Furthermore, the study suggests that the incorporation of TiO_2 NPs enhances sensitivity to ultrasound stimulation, thereby increasing the release rate of therapeutic factors. Overall, the dual-stimulus system studied here holds promise for new applications in therapeutic delivery in a relatively inexpensive and minimally invasive manner.

In conclusion, the present study demonstrated CS/β-GP/TiO_2 NPs as composite hydrogels that are injectable, biocompatible, and thermosensitive systems suitable for ultrasound-triggered

drug release. Furthermore, all hydrogels gelated at temperatures close to 37˚C, enabling *in situ* gelation upon delivery to the body, and possessed the required injectability for minimally invasive delivery. Compared with the control group, the hydrogels exhibited the ability to promote sustained delivery of NaF and BSA drug mimics, with enhanced release achieved under all circumstances owing to ultrasound application. Importantly, hydrogel groups containing TiO_2 NPs demonstrated higher levels of release after ultrasound treatment than pure hydrogels, confirming that TiO_2 NPs increased the sensitivity of the thermos-responsive hydrogel to ultrasound stimulation. Ultrasound-triggered thermos-responsive hydrogels are promising for drug delivery applications.

The present study primarily focused on the validation of ultrasound-triggered drug release. While drug release under ultrasound activation was observed, the authors have not yet delved into specific release mechanisms, such as thermal effects or cavitation. Therefore, future research will emphasize this aspect to gain a deeper understanding of the mechanisms behind ultrasound-triggered drug release and its applications in drug delivery systems.

To this end, the authors plan to apply for the ethical approval required to conduct animal experiments, ensuring the compliance and scientific integrity of the present study. These experiments will provide deeper insights, helping to validate the behavior of hydrogels *in vivo* and their impact on drug release. A series of experiments will be designed to evaluate the effects of hydrogel materials on major organs (heart, liver, lungs, kidneys). Specifically, future research will focus on the following aspects: i) Histopathological analysis: By preparing tissue sections and utilizing microscopy, the impact of hydrogel materials on the structural integrity of major organ tissues will be assessed. ii) Physiological parameter monitoring: Physiological parameters, such as heart rate and respiratory rate, will be recorded throughout the experimental period to evaluate the biocompatibility and safety of the materials. iii) Biochemical indicator assessment: Routine blood tests will be conducted to monitor changes in biomarkers (such as liver and kidney function) to assess the overall health effects of the materials on the animals.

The aim of these future experiments will be to gain a comprehensive understanding of the mechanisms of ultrasound-triggered drug release and its biocompatibility, laying the groundwork for future clinical applications. The authors look forward to further exploring and validating these critical factors in their future research to advance the development of ultrasound-triggered drug delivery systems.

Acknowledgements

Not applicable.

Funding

No funding was received.

Availability of data and materials

The data generated in the present study may be requested from the corresponding author.

Authors' contributions

YZ was responsible for conceptualization, investigation, and writing the original draft as well as reviewing and editing the manuscript. YRY designed the experimental methods and performed the analysis of results using software. YX contributed through data curation and preparation of experimental materials (resources). XR focused on visualization of results, also prepared experimental materials and acquired the data. YFQ was in charge of validation and formal analysis. TYQ oversaw supervision, project administration, funding acquisition and data collection. YX, XR, YFQ and TYQ confirm the authenticity of all the raw data. All authors read and approved the final manuscript.

Ethics approval and consent to participate

Not applicable.

Patient consent for publication

Not applicable.

Competing interests

The authors declare that they have no competing interests.

References

1. Shamay Y, Adar L, Ashkenasy G and David A: Light induced drug delivery into cancer cells. Biomaterials 32: 1377-1386, 2011.
2. Chao Y, Chen Q and Liu Z: Smart injectable hydrogels for cancer immunotherapy. Adv Funct Mater 30: 1902785, 2020.
3. Bertsch P, Diba M, Mooney DJ and Leeuwenburgh SCG: Self-healing injectable hydrogels for tissue regeneration. Chem Rev 123: 834-873, 2022.
4. Abdollahi A, Roghani-Mamaqani H, Razavi B and Salami-Kalajahi M: The light-controlling of temperature-responsivity in stimuli-responsive polymers. Polym Chem 10: 5686-5720, 2019.
5. Lee SY, Yang M, Seo JH, Jeong DI, Hwang C, Kim HJ, Lee J, Lee K, Park J and Cho HJ. Serially pH-modulated hydrogels based on boronate ester and polydopamine linkages for local cancer therapy. ACS Appl Mater Interfaces 13: 2189-2203, 2021.
6. Lin X, Song J, Chen X and Yang H: Ultrasound-activated sensitizers and applications. Angew Chem Int Ed Engl 59: 14212-14233, 2020.
7. Wu J, Zheng K, Huang X, Liu J, Liu H, Boccaccini AR, Wan Y, Guo X and Shao Z: Thermally triggered injectable chitosan/silk fibroin/bioactive glass nanoparticle hydrogels for in-situ bone formation in rat calvarial bone defects. Acta Biomater 91: 60-71, 2019.
8. Kim G, Wu Q, Chu JL, Smith EJ, Oelze ML, Moore JS and Li KC Ultrasound controlled mechanophore activation in hydrogels for cancer therapy. Proc NatI Acad Sci USA 119: e2109791119, 2022.
9. Liu H, Wang C, Li C, Qin Y, Wang Z, Yang F, Li Z and Wang J: A functional chitosan-based hydrogel as a wound dressing and drug delivery system in the treatment of wound healing. RSC Adv 8: 7533-7549, 2018.
10. Son S, Kim JH, Wang X, Zhang C, Yoon SA, Shin J, Sharma A, Lee MH, Cheng L, Wu J and Kim JS: Multifunctional sonosensitizers in sonodynamic cancer therapy. Chem Soc Rev 49: 3244-3261, 2020.
11. Yu S, Zheng J, Xie H, Deng Q, Wang J, Chen J, Zhou H and Wang J: Biocompatible hydrogel nanoparticles with lysosomal escape properties for the delivery of siRNA for the gene therapy of colorectal carcinoma. ACS Appl Nano Mater 7: 6612-6625, 2024.
12. Qi F, Li H, Wang Y and Ding C: Responsive DNA hydrogels: Design strategies and prospects in biosensing. Chem Commun 60: 11744-11751, 2024.

13. Wang S: Soft hydrogel semiconductors with augmented biointeractive functions. Science 377: eadp9314, 2024.
14. Wei X, Li H and Yue W: A highly linear stretchable MXene-based biocompatible hydrogel-elastomer hybrid for organ monitoring. Sci China Materials 67: 2956-2968, 2024 (In Chinese).
15. Huebsch N, Kearney CJ, Zhao X, Kim J, Cezar CA, Suo Z and Mooney DJ: Ultrasound-triggered disruption and self-healing of reversibly cross-linked hydrogels for drug delivery and enhanced chemotherapy. Proc Natl Acad Sci USA 111: 9762-9767, 2014.
16. Levingstone T, Ali B, Kearney C and Dunne N: Hydroxyapatite sonosensitization of ultrasound-triggered, thermally responsive hydrogels: An on-demand delivery system for bone repair applications. J Biomed Mater Res B, Appl Biomater 109: 1622-1633, 2021.
17. MacDonald V, Wilson K, Sonne MWL and Keir PJ: Grip type alters maximal pinch forces in syringe use. Hum Factors 59: 1088-1095, 2017.
18. Elisa L and Filippo R: Polymer-based thermoresponsive hydrogels for controlled drug delivery. Exp Opin Drug Deliv 19: 1203-1215, 2022.
19. Khan MUA, Stojanović GM, Abdullah MFB, Dolatshahi-Pirouz A, Marei HE, Ashammakhi N and Hasan A: Fundamental properties of smart hydrogels for tissue engineering applications: A review. Int J Biol Macromol 254: 127882-127882, 2023.
20. Zhao F, Liu M, Guo H, Wang Y, Zhang Y, He M and Cai Z: Stimuli-responsive hydrogels based on protein/peptide and their sensing applications. Prog Mater Sci 148: 101355, 2025.
21. Liu W, Borrell MA, Venerus DC, Mieler WF and Kang-Mieler JJ: Characterization of biodegradable microsphere-hydrogel ocular drug delivery system for controlled and extended release of Ranibizumab. Transl Vis Sci Technol 8: 12, 2019.
22. Zhou X, He X, Shi K, Yuan L, Yang Y, Liu Q, Ming Y, Yi C and Qian Z: Injectable thermosensitive hydrogel containing erlotinib-loaded hollow mesoporous silica nanoparticles as a localized drug delivery system for NSCLC therapy. Adv Sci 7: 2001442, 2020.
23. Amini-Fazl MS, Mohammadi R and Kheiri K: 5-Fluorouracil loaded chitosan/polyacrylic acid/Fe3O4 magnetic nanocomposite hydrogel as a potential anticancer drug delivery system. Int J Biol Macromol 132: 506-513, 2019.
24. Mathew AP, Uthaman S, Cho KH, Cho CS and Park IK: Injectable hydrogels for delivering biotherapeutic molecules. Int J Biol Macromol 110: 17-29, 2018.
25. Kim J, Choi Y, Kim DH, Yoon HY and Kim K: Injectable hydrogel-based combination cancer immunotherapy for overcoming localized therapeutic efficacy. Pharmaceutics 14: 1908, 2022.
26. Sundararaj SC, Thomas MV, Dziubla TD and Puleo DA: Bioerodible system for sequential release of multiple drugs. Acta Biomater 10: 115-125, 2014.
27. El-Husseiny HM, Mady EA, El-Dakroury WA, Doghish AS and Tanaka R: Stimuli-responsive hydrogels: Smart state of-the-art platforms for cardiac tissue engineering. Front Bioeng Biotechnol 11: 1174075, 2023.
28. Jiménez-Gómez CP and Cecilia JA: Chitosan: A natural biopolymer with a wide and varied range of applications. Molecules 25: 3981, 2020.